Comparison between the Performances of a Well-Stirred Slurry Reactor and a Spray Loop Reactor for the Alkylation of p-Cresol with Isobutene

ARTICLE *in* INDUSTRIAL & ENGINEERING CHEMISTRY RESEARCH · AUGUST 2005

Impact Factor: 2.59 · DOI: 10.1021/ie050221j

4 AUTHORS:

E. Santacesaria
University of Naples Federico II
199 PUBLICATIONS **3,830** CITATIONS
SEE PROFILE

Martino Di Serio
University of Naples Federico II
155 PUBLICATIONS **2,886** CITATIONS
SEE PROFILE

Riccardo Tesser
University of Naples Federico II
90 PUBLICATIONS **1,949** CITATIONS
SEE PROFILE

Francesco Cammarota
Italian National Research Council
32 PUBLICATIONS **340** CITATIONS
SEE PROFILE

Comparison between the Performances of a Well-Stirred Slurry Reactor and a Spray Loop Reactor for the Alkylation of *p*-Cresol with Isobutene

Elio Santacesaria,* Martino Di Serio, Riccardo Tesser, and Francesco Cammarota

Università di Napoli - Dipartimento di Chimica-Via Cinthia - Complesso Universitario di Monte S. Angelo, 80126 - Napoli - Italy

The kinetics of the alkylation of *p*-cresol with isobutene has been studied, first of all, in a well-stirred slurry reactor. Preliminary runs of CO_2 absorption in water and of isobutene absorption in *p*-cresol, in the same reactor, have been made for estimating the gas−liquid mass-transfer coefficient in an independent way. The kinetic model, developed in a previous work, has been improved and the related parameters have been determined by mathematical regression analysis of many kinetic runs. Different kinetic runs have then been performed also by using a spray tower loop reactor (STLR) in similar physical conditions. These runs have been simulated in a satisfactory way by using the same kinetic model and parameters, changing only mass-transfer parameters for taking into account the different fluid dynamic conditions. The performances obtained by the two different reactors are in some conditions comparable. This work has demonstrated, therefore, the possibility and the convenience of extending the use of STLR reactors in performing gas−liquid−solid reactions.

Introduction

The behavior of multiphase reactors is often strongly affected by mass-transfer limitations, and different types of reactor configurations (bubble columns, jet loop reactors, spray tower loop reactors, and mechanically agitated reactors) are employed, depending on the characteristics of the reactions. Spray tower loop reactors (STLR) are largely employed for very fast reactions, such as neutralization reactions or pollutant abatement by absorption from gaseous mixtures. One of the main applications for spray contactors, for example, is in gas stream desulfurization.[1]

It is important to point out that in STLR reactors the liquid is the dispersed phase instead of the gaseous one, as it occurs in the other mentioned reactors. The role of the mass-transfer limitations in these conditions have been poorly investigated in the literature.[2−7]

In a previous work[6] we have shown that a STLR reactor can be conveniently used for some gas−liquid reactions provided that the solubility of the gaseous reagent is high enough. In particular we have studied the ethoxylation of different organic substrates,[8−11] and we concluded that, for moderately fast reactions (with Hatta no. $\cong$ 1), the use of a STLR reactor can be more convenient than one of the other reactors, such as, for example bubble columns or well-stirred reactors. As a matter of fact, we have found that the gas−liquid mass-transfer rate in a STLR reactor is very high when a suitable spray nozzle is used and the behavior of the reactor can be interpreted with a mathematical model that assumes the produced droplets are internally well-mixed.[6] Moreover, we have evidence that, in some cases, the spray tower loop reactors can give better performances of the mechanically agitated reactors with the advantage of the absence of any rotating device and with the possibility of operating easily also at high pressure. A further positive aspect of the STLR reactor is the separation existing between the mass-transfer zone and the reaction one, inside the reactor, in the presence of a moderately fast gas−liquid reaction, and this is an element of greater flexibility.

In the present work, we have studied the possibility of extending the use of the STLR reactor also to gas−liquid−solid reactions. No paper has been published exploring this possibility. We will consider here and discuss all the possible constraints in the use of a STLR reactor in performing gas−liquid−solid reactions, by examining also the possible advantages and drawbacks of the proposed technique. To do this, we have chosen for our investigation the alkylation of *p*-cresol with isobutene as a test reaction. This reaction, catalyzed by acid exchange resins, occurs in two consecutive steps,[12,13] the first giving 2-*tert*-butyl-*p*-cresol (M) and the second 2,6 di-*tert*-butyl-*p*-cresol (BHT). Isobutene can also give place to oligomers as side products and, normally, only dimerization (D) and trimerization (T) occur.

In the present work, the reaction has been performed in both a well-mixed gas−liquid−solid reactor and in a spray tower loop reactor. The kinetic model developed in a previous work[12] has been improved in view of a possible scale-up, and more reliable kinetic parameters have been determined by mathematical regression analysis on many more kinetic runs performed in the slurry reactor. The same kinetic model has also been successfully used for simulating the kinetic runs performed in the STLR reactor. The performances of the two reactors have then been compared with particular attention devoted to the effect of mass-transfer limitations. A preliminary fluid dynamic characterization has been performed for both of the reactors by studying the physical absorption of CO_2 in water.

Experimental Section

Apparatus, Methods, and Reagents. Two different reactors have been used for studying the kinetics and

* To whom correspondence must be addressed. E-mail: santacesaria@chemistry.unina.it.

10.1021/ie050221j CCC: $30.25
Published on Web 08/06/2005

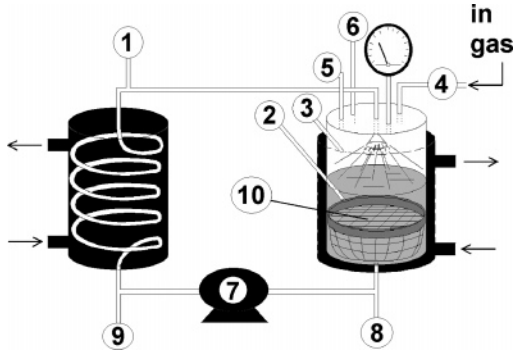

Figure 1. Scheme of the used spray tower loop reactor: (1) sampling line; (2) liquid temperature measurement; (3) gas temperature measurement; (4) flow meter; (5) pressure transducer; (6) safety valve; (7) gear pump; (8, 9) drain line; (10) catalyst basket.

mass transfer of the alkylation of *p*-cresol, a well-mixed slurry reactor, similar to the one used in a previous work[12] and a spray tower loop reactor, schematized in Figure 1.

The well-mixed slurry reactor is a jacketed stainless steel cylindrical reactor equipped with a magnetically driven stirrer, consisting of a turbine connected to a holed rod and able to develop a great interface area. The internal diameter of the reactor was 7.5 cm and the height 14 cm, while the diameter of the impeller was 2.5 cm. The reactor was thermostated with oil recirculation. The control of the pressure, temperature, and isobutene feeding the reactor was fully automated by an Analog Device system. The overall volume of the reactor was about 620 cm^3 and was normally loaded with 140 cm^3 of *p*-cresol. After the introduction of the catalyst and of the *p*-cresol reagent, the reactor was purged with nitrogen, at atmospheric pressure and under moderate stirring, and heated. When the reaction temperature was reached, the reactor was evacuated with a vacuum pump and then loaded with isobutene. The pressure of isobutene was kept constant at about 1 atm. Samples of the liquid reaction mixture were withdrawn, from the top of the reactor, at different times and gas-chromatographically analyzed. Analyses were performed by using an HP-5 column (30 m−0.32 mm−1.05 μm) and a flame ionization detector (FID). Hydrogen has been used as carrier gas. The temperature of the column has been programmed with the following sequence: 40 °C for 2 min, which then was increased with a scanning rate of 20 °C/min until it reached 260 °C and was kept at this temperature for 1 min.

The spray tower loop reactor of Figure 1 is a jacketed stainless steel reactor with a spray nozzle mounted on the top of the reactor. The used spray nozzle was a full cone nozzle with a spray angle of 90° in AISI316 furnished by PNR Italia (Nozzle Code DAU.1118.B3.PNR), giving, in optimal condition, water droplets with $D_{32} \cong 136$ μm. This optimal condition is reached for a pressure drop across the nozzle of 3.0 bar. This condition corresponds to a water flow rate of about 1.2 L/min. A basket of a closely woven wire net entrapping the catalyst has been located at the bottom of the reactor. The internal diameter of the reactor was 12.2 cm, while the height, 34 cm. The catalyst basket had a maximum diameter of 11.5 cm, and the catalytic bed inside the basket had a height of 0.57 cm corresponding to 35 g of catalyst and 1.13 cm for 70 g of catalyst. The overall volume of the reactor was about 4000 cm^3, normally, loaded with 500 cm^3 of *p*-cresol that is a quantity enough to completely submerge the catalyst basket. The reactor is batchwise-operated for what concerns the liquid phase (*p*-cresol), while the gaseous reactant (isobutene) is semi-continuously fed to the reactor.

Table 1. Main Properties of the Cationic Resin Used as Catalyst

catalyst commercial name	Amberlyst 15 (by Rohm & Haas Co.)
mean diameter	0.07 cm
bed density	0.595 g/cm^3
acidity	4.47 meq/g
specific surface	45 m^2/g
porosity	0.33
pore diameter	200−600 Å

Table 2. List of the Kinetic Runs Performed in the Well-Stirred Slurry Reactor

run	temp (°C)	isobutene pressure (atm)	catalyst amt (g)	*p*-cresol (g)
A1	50	1	20	140
A2	60	1	10	140
A3	72	1	10	140
A4	40	1	10	140
A5	50	1	10	140

The liquid drops emerging from the spray nozzle and dispersed in the gas phase absorbs isobutene until reaching the solubility saturation. Dissolved isobutene then reacts on the catalyst surface, and the liquid, depleted of isobutene, is recycled to the spray nozzle. The liquid inlet temperature is adjusted by a heat exchanger kept at constant temperature. Also in this case, after the introduction of the reagent *p*-cresol and catalyst, the reactor was purged with nitrogen at atmospheric pressure and heated at the reaction temperature. Then nitrogen was eliminated by vacuum and isobutene was loaded at the desired initial pressure. The isobutene consumed by the reaction was automatically replaced by keeping constant the initial pressure. Samples of the liquid reaction mixture were withdrawn, from the recirculating line, at different times and gas-chromatographically analyzed, as previously seen. Also in this case, the control of the pressure, temperature, and isobutene feeding the reactor was fully automated by an Analog Device system. The employed catalyst was a cationic resin of the Rohm and Haas Co. (Amberlyst 15) whose main properties are summarized in Table 1. Before the use, the catalyst was dried for 6 h at 100 °C in a ventilated oven in order to remove adsorbed water. Reagents used have been purchased by Sigma Aldrich at the highest level of purity available (cresol, 99 wt %) with the exception of isobutene furnished by SON SpA (>99.9 vol %).

Kinetic runs in the well-mixed slurry reactor have been performed at different temperatures and catalyst concentrations but taking constant the isobutene pressure at 1 bar, as can be seen in Table 2. In the case of the spray tower loop reactor, kinetic runs have been performed by changing the temperature, catalyst concentration, pressure, and liquid recirculation flow rate, as reported in Table 3.

Fluid dynamic characterization of both reactors have been made by physical absorption of CO_2 in water in order to estimate gas−liquid mass-transfer parameters, in an independent way and in the absence of chemical reaction.

Vapor−liquid equilibria of isobutene in binary mixtures with respectively *p*-cresol and the main products

Table 3. List of the Kinetic Runs Performed in the Spray Tower Loop Reactor

run	temp (°C)	isobutene pressure (atm)	Amberlyst (g)	*p*-cresol (g)	recycle flow rate (L/min)
B1	60	1	35	500	1.2
B2	72	1	35	500	1.2
B3	72	1.3	70	500	1.63
B4	60	1	70	500	1.63
B5	60	2.5	70	500	1.63

M and BHT, useful for determining isobutene concentration in the liquid bulk and on the surface catalyst, have been studied in a previous work, and activity coefficients have already been determined in that work.[12]

Results

Kinetics and Mass-Transfer Runs Performed in the Well-Stirred Slurry Reactor. An estimation of the gas−liquid mass-transfer coefficient in the adopted well-stirred slurry reactor has been made by performing, first of all, different runs of CO_2 absorption in water at different stirring rates. Each run consists of observing the evolution with time of the amount of absorbed CO_2. By considering only the liquid side mass-transfer resistance, we can write

$$\frac{dC_{CO_2}}{dt} = K_L a_L (C^*_{CO_2} - C_{CO_2}) = \beta_L (C^*_{CO_2} - C_{CO_2}) \quad (1)$$

by integrating:

$$\ln \frac{(C^*_{CO_2} - C_{CO_2})}{C^*_{CO_2}} = -\beta_L t \quad (2)$$

Data of CO_2 solubility in water, at 25 °C, corresponding to $C^*_{CO_2}$, can be derived from the literature.[14,15] In Figure 2 the linear trends obtained for $\ln[(C^*_{CO_2} - C_{CO_2})/C^*_{CO_2}]$ versus t are reported. β_L values can be obtained from the related slopes.

The effect of the stirring rate on β_L can be better appreciated by putting the values obtained as a function of stirring rates, as reported in Figure 3.

As can be seen, with the used reactor a threshold value of 600−700 rpm is necessary for the development of the interfacial area. At stirring rates higher than 1800 rpm there is no further increase in the β_L value, and for this reason we decided to work at 1800 rpm. Then, a similar run of physical absorption has also been made by absorbing isobutene, at 40°C, in *p*-cresol, stirring at 1800 rpm. A 140 g amount of *p*-cresol was charged in the reactor and contacted with isobutene at 1 atm. The amount of absorbed isobutene along the time has been determined, and data obtained have been arranged in a plot similar to the one reported in Figure 2 for determining β_L in conditions similar to the ones used in the reaction. The isobutene concentration has been determined by applying the Antoine relation for determining the vapor pressure and the Raoult law for evaluating the molar fraction and hence the concentration. The obtained value of $\beta_L = 0.047\ s^{-1}$ is reported in Figure 3 for a comparison with the system CO_2−water. The observed difference is consistent with the difference between the molecular diffusion coefficients for respectively CO_2 in water ($D_{CO_2/H_2O} = 1.9 \times 10^{-5}$ cm^2/s)[16] and

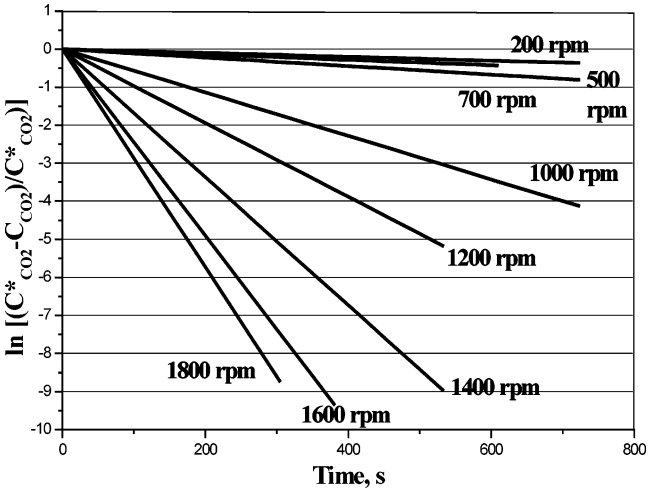

Figure 2. Effect of stirring rate on the gas−liquid mass-transfer parameter β_L.

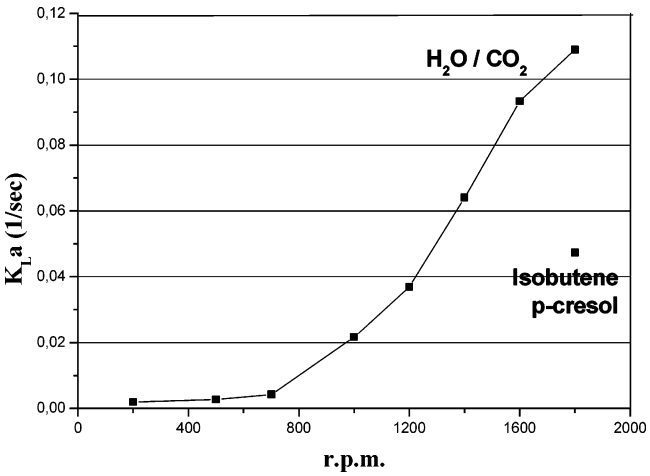

Figure 3. Evolution of β_L with the stirring rate: β_L for isobutene in *p*-cresol.

isobutene in *p*-cresol ($D_{isob/p\text{-cresol}} = 0.6 \times 10^{-5}$ cm^2/s). The last value has been estimated by using the Wilke and Chang[17] relation:

$$D_{12} = (7.4 \times 10^{-8}) \frac{T(\chi M_2)^{0.5}}{\mu V_B^{0.6}} \quad (3)$$

This relation has also been used for estimating the change of β_L with temperature, considering also the variation of *p*-cresol viscosity. In agreement with these findings, we have also observed that kinetic parameters were not affected by β_L values greater than the one reported for isobutene in Figure 3 evaluated at 1800 rpm; that is, gas−liquid mass-transfer was not limiting at the adopted stirring rate.

The kinetic runs performed in the well-stirred slurry reactor are listed in Table 2 together with the adopted operative conditions. As before mentioned, the kinetic model adopted for simulating the runs has been improved with respect to the one reported in a previous work[12] and structured in a more general way, allowing reactor scale-up simulation. Mass-transfer parameters have been clearly changed, because the reactor is different. Kinetic parameters have been recalculated by mathematical regression analysis[18] on a more relevant number of kinetic runs and are, therefore, more reliable than the ones of the previous work. We summarize here

the main aspects of the adopted kinetic model and related modifications introduced.

The alkylation of *p*-cresol with isobutene for obtaining the antioxidant BHT occurs in two steps that are

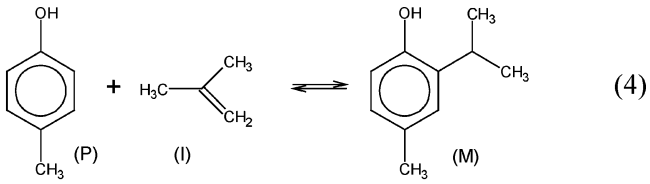

(4)

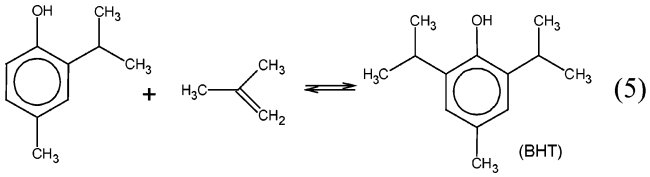

(5)

As mentioned before, also isobutene oligomerizations occur as side reactions, such as

(6)

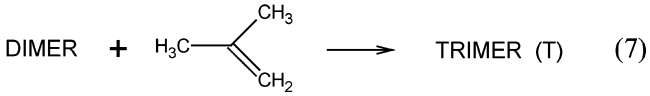

(7)

We can write more simply

(1)	$P + I \rightleftarrows M$	monoalkylation	r_1
(2)	$M + I \rightleftarrows BHT$	dialkylation	r_2
(3)	$2I \rightarrow D$	dimerization	r_3
(4)	$D + I \rightarrow T$	trimerization	r_4

The following expressions for the reaction rates can reasonably be applied:

$$r_1 = \eta k_1 \left(C_{Ps} C_{Is} - \frac{C_{Ms}}{K_{e1}} \right) C_{cat.} S_{spec} \tag{8}$$

$$r_2 = \eta k_2 \left(C_{Ms} C_{Is} - \frac{C_{Bs}}{K_{e2}} \right) C_{cat.} S_{spec} \tag{9}$$

$$r_3 = \eta k_3 C_{Is}^{\,2} C_{cat.} S_{spec} \tag{10}$$

$$r_4 = \eta k_4 C_{Is} C_{Ds} C_{cat.} S_{spec} \tag{11}$$

Isobutene has been assumed as a reference component for the calculation of the effectiveness factor, because its concentration is small with respect to the other reagents. Catalyst effectiveness factor is then evaluated as a function of concentrations and diffusivity at any step of integration; that is, it has not been considered an adjustable parameter for data fitting. For simplifying the calculation a pseudo-first-order model has been assumed by considering constant the concentration of P and M during each integration step. The contributions in the calculation of the Thiele modulus for the formation of D and T have been neglected because related reaction rates are normally quite low.

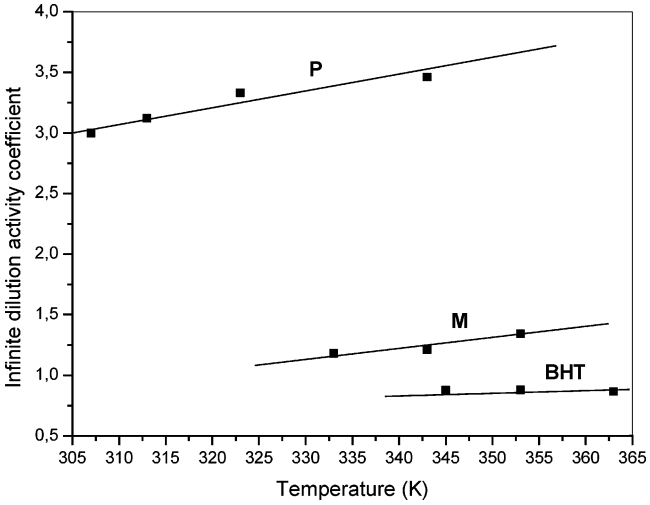

Figure 4. Infinite dilution activity coefficients as a function of temperature for *p*-cresol (P), monoalkylate (M), and dialkylate (BHT).

Also the contribution of the reverse reactions in r_1 and r_2 has been ignored. Therefore, Thiele modulus has been calculated as

$$\Phi = R_P \sqrt{\frac{(k_1 C_P + k_2 C_M) C_{cat.} S_{spec}}{D_{eff}}} \tag{12}$$

D_{eff} has been estimated in the usual way by using the following relationship:[19]

$$D_{eff} = \frac{D \epsilon_p}{\tau} = 0.15 D \tag{13}$$

According to Satterfield[19] we have assumed a value of 2 for the tortuosity factor of the exchange resin catalyst. At 50−70 °C, D_{eff} resulted in about 1×10^{-6} cm^2/s.

The isobutene partition is affected by nonideality of this key component dissolved in the reaction mixture, this last changing along with time. For the evaluation of isobutene solubility also the effects of operative pressure and of nonideality have been taken into account in the phase partition calculation. The activity coefficients can be determined from the infinite dilution activity coefficients of binary systems, experimentally determined in the already mentioned previous work[12] and are reported in the plot of Figure 4 as a function of the temperature.

The isobutene activity coefficients have been determined by using the relationship:[12]

$$\overline{\gamma}_I = \exp(1 - x_I)^2 \ln \overline{\gamma_I^{inf}} \tag{14}$$

The calculation of the isobutene concentration, at the solid surface, can be made by applying a pseudo-steady-state condition for respectively the gas−liquid and liquid−solid mass-transfer rates and reaction rates, that is, from the following two relationships:

$$K_L a_L (C_I - C_{Ib}) - K_S a_S (C_{Ib} - C_{Is}) = 0 \tag{15}$$

$$K_S a_S (C_{Ib} - C_{Is}) - (r_1 + r_2 + 2r_3 + r_4) = 0 \tag{16}$$

By opportunely developing the two relations (15) and (16), we obtain C_{Is} as

$$C_{Is} = \frac{-(b - \beta R_N) \pm \sqrt{(b - \beta R_N)^2 + 4a(d + \beta R_M C_I)}}{2a} \tag{17}$$

where

$$a = 2\eta k_3 \tag{18}$$

$$b = \eta k_1 C_P + \eta k_2 C_M + \eta k_4 C_D + \beta \tag{19}$$

$$d = \eta k_1 \frac{C_M}{K_{e1}} + \eta k_2 \frac{C_B}{K_{e2}} \tag{20}$$

$$\beta = \frac{K_S a_S}{C_{cat.} S_{spec}} \tag{21}$$

$$R_M = \frac{\alpha}{1 + \alpha} \tag{22}$$

$$R_N = \frac{1}{1 + \alpha} \tag{23}$$

$$\alpha = \frac{K_L a_L}{K_S a_S} \tag{24}$$

The evolution with time of the reagents and products can be determined by integrating the following kinetic equations, taking into account also for the isobutene nonideality in the reacting mixture and for the change of the liquid volume by adjusting after each step of integration both the corresponding values.

$$\frac{dC_P}{dt} = -r_1 \tag{25}$$

$$\frac{dC_M}{dt} = r_1 - r_2 \tag{26}$$

$$\frac{dC_B}{dt} = r_2 \tag{27}$$

$$\frac{dC_D}{dt} = r_3 - r_4 \tag{28}$$

$$\frac{dC_T}{dt} = r_4 \tag{29}$$

$$-\frac{1}{V_L}\frac{dn_I}{dt} = (r_1 + r_2 + 2r_3 + r_4) \tag{30}$$

By submitting to mathematical regression analysis[18] the kinetic runs of Table 2, reported in Figures 5−9, a satisfactory fitting is obtained with the parameters reported in Table 4, as can be appreciated in the mentioned figures.

Kinetics and Mass Transfer in a Spray Tower Loop Reactor. Different runs have been performed in the described spray tower loop reactor by adopting operative conditions similar to the ones used in the slurry reactor, that is the same temperatures and catalyst concentrations. Initial liquid volumes have been, on the contrary, greatly increased from 140 to 500 cm^3. The kinetic runs performed are summarized in Table 3 together with the operative conditions:

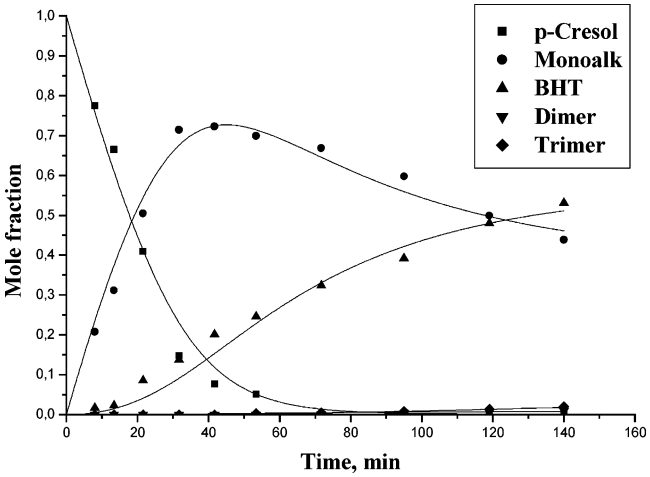

Figure 5. Kinetic run simulation: run A1 in Table 2.

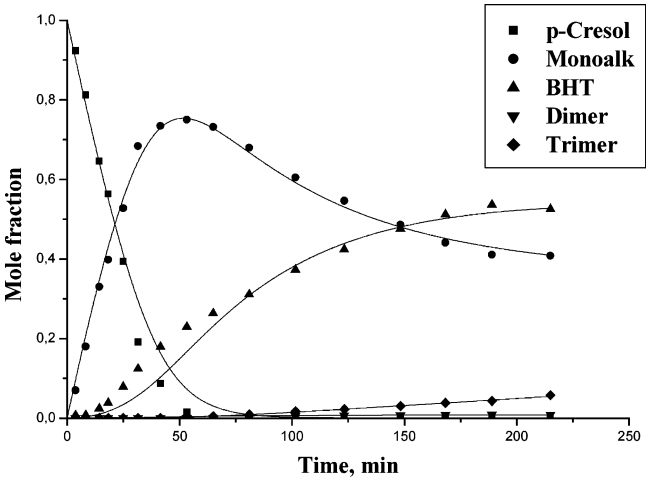

Figure 6. Kinetic run simulation: run A2 of Table 2.

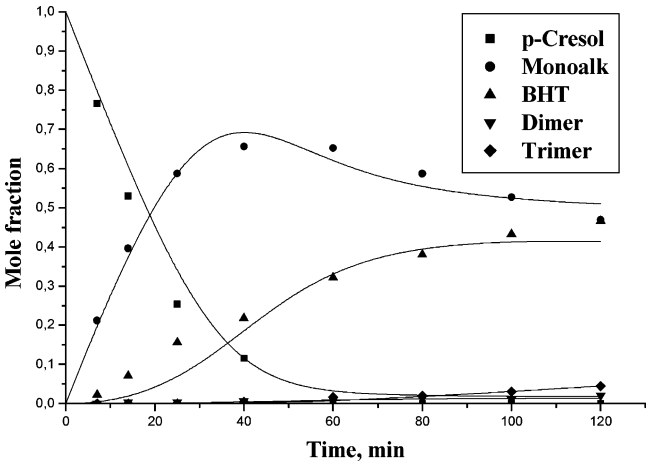

Figure 7. Kinetic run simulation: run A3 of Table 2.

As can be seen, in Figures 10−14, the STLR reactor has lower performances at the lowest temperature of 60 °C, while the performances, at 72 °C, are comparable for what concerns the reaction time with respect to the slurry reactor. This behavior can be interpreted by assuming that at the lowest temperature the spray nozzle is not efficient enough in producing very small droplets for the high viscosity of the liquid. Consider that *p*-cresol melting point is about 30 °C. At 72 °C, the rate of *p*-cresol disappearing is about the same in the two reactors and also the other reactions occur in a

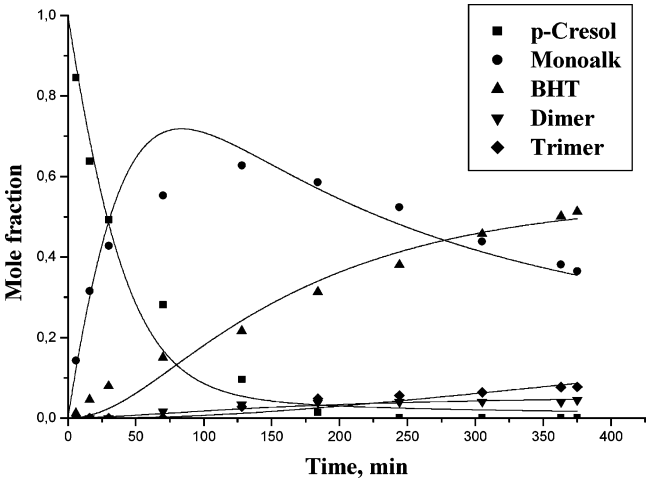

Figure 8. Kinetic run simulation: run A4 of Table 2.

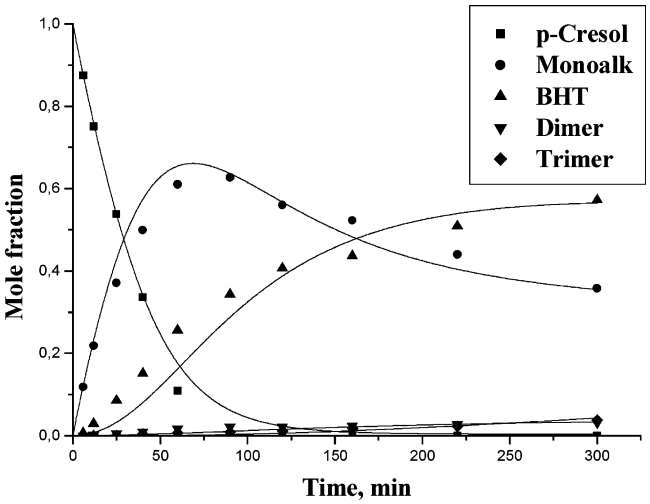

Figure 9. Kinetic run simulation: run A5 of Table 2.

Table 4. Kinetic and Equilibrium Parameters Obtained by Mathematical Regression Analysis

	ln k^0_i or $K_{eq2}{}^{0\,a}$	ΔE_i or ΔH (cal/mol)
k_1	19.52 ± 1.16	18703 ± 612
k_2	21.00 ± 1.47	20862 ± 584
k_3	23.90 ± 2.48	22507 ± 983
k_4	24.54 ± 1.92	21448 ± 756
K_{eq1}	20.50 ± 2.57	6826 ± 1568
K_{eq2}	6.74 ± 1.34	−647 ± 256

[a] $k_i = k_i{}^0 \exp(-\Delta E_i/RT)$, cm^4/(s mol). $K_{eq2} = K_{eq2}{}^0 \exp(-\Delta H/RT)$, cm^3/mol.

comparable time. Although the two reactors could seem very different and not directly comparable, when the residence time of the liquid on the catalytic bed of the STLR reactor gives place to a low conversion and the recycle flow rate is high, STLR reactor can be considered as a well-mixed reactor. At this purpose, it is possible to estimate that the conversion of *p*-cresol, occurring for each loop of the liquid volume on the catalyst, is about 1%, that is, low enough to consider the reactor well-mixed. To simulate the reactor, it is necessary to consider that drops emerging from the spray nozzles are almost completely saturated at 72 °C. Therefore, the gas−liquid mass-transfer contribution can be neglected. On the contrary, the liquid−solid mass-transfer rate assumes a great relevance in this type of reactors, strongly depending on the linear velocity of the liquid fluid passing across the catalytic bed.[20,21] Simulations

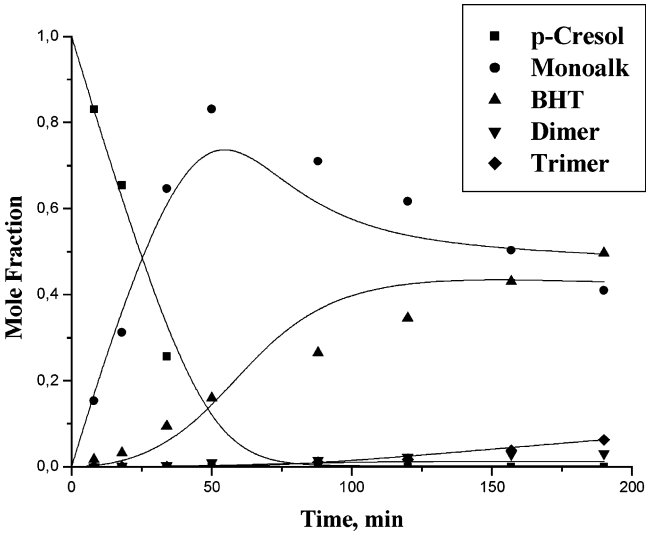

Figure 10. Kinetic run simulation: run B2 of Table 3.

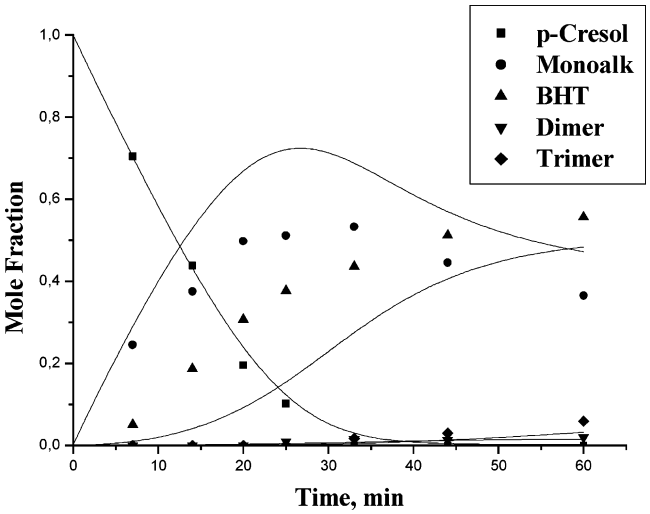

Figure 11. Kinetic run simulation: run B3 of Table 3.

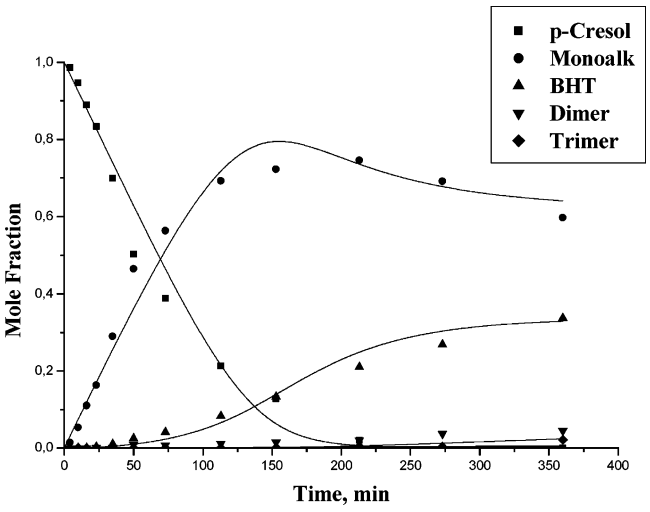

Figure 12. Kinetic run simulation: run B1 of Table 3.

obtained, at 72 °C, by using the optimized values of K_s reported in Table 5, can be seen in Figures 10 and 11. For simulating runs performed at 60 °C, it is reasonable to assume a partial saturation of the liquid reagents with isobutene. The partial saturation can be estimated always by regression analysis, and it corresponds to

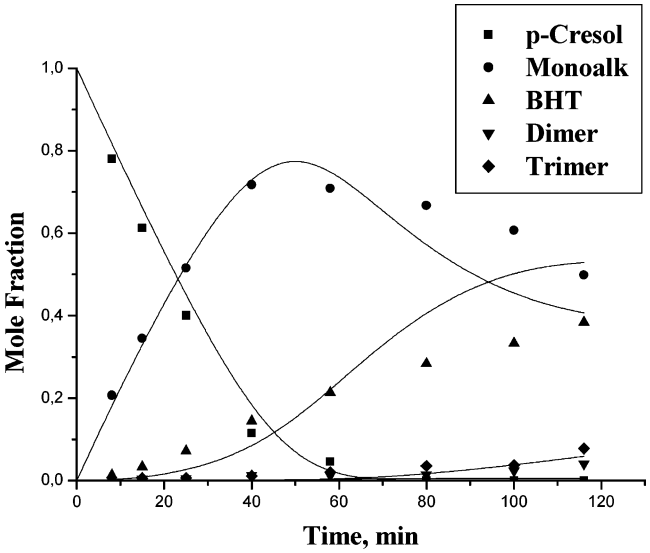

Figure 13. Kinetic run simulation: run B4 of Table 3.

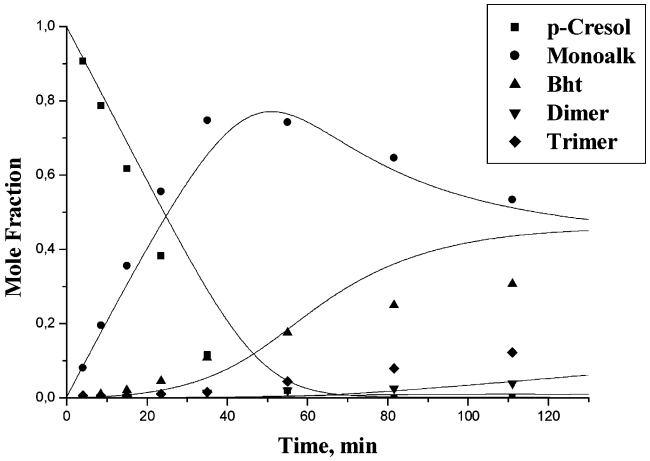

Figure 14. Kinetic run simulation: run B5 of Table 3.

Table 5. Mass-Transfer Parameters Obtained Both by Mathematical Regression Analysis and from the Use of Literature Correlations

run	K_S (by regression)	K_S (eq 33)[19]	K_S (eq 34)[20]
B1	0.9×10^{-3}	1.1×10^{-3}	1.0×10^{-3}
B2	3.4×10^{-3}	1.5×10^{-3}	1.4×10^{-3}
B3	3.0×10^{-3}	1.8×10^{-3}	1.6×10^{-3}
B4	1.8×10^{-3}	1.2×10^{-3}	1.2×10^{-3}
B5	0.5×10^{-3}	1.2×10^{-3}	1.2×10^{-3}

about 80% of saturation. Simulation results with the optimized value of K_s reported in Table 5 can be appreciated in Figures 12−14.

Discussion and Conclusions

By observing the performances obtained with the STLR reactor, reported in Figures 10−14, in comparison with the ones obtained in the well-mixed slurry reactor and reported in Figures 5−9, it can be noted that runs performed in the STLR reactor, at the lowest temperature of 60 °C, are much slower than the ones performed in the slurry reactor, in the same conditions of temperature and catalyst concentration (compare, for example run A2 with B1). We attributed, first of all, this difference to the difficulty of the spray nozzle in dispersing *p*-cresol having, at 60 °C, a viscosity 6 times greater than that of water. However, we have seen that by considering results at 60 °C the achievement of a saturation level of about 80% of the total is enough to simulate the runs with the same kinetic parameters derived from the slurry reactor. This is potentially a drawback in the use of a STLR reactor, requiring liquid properties not contrasting the formation of small droplets. However, by increasing the temperature only 12 °C, this inconvenience is vanished and the STLR reactor performances obtained at 72 °C are comparable with the ones of the well-stirred slurry reactor, operating at the same temperature and with the same catalyst concentration (compare run A3 with run B2). As we have simulated the STLR reactor by considering the liquid phase well-mixed, the obtained results should be very similar to the ones of a slurry reactor in which the liquid phase is completely saturated, that is, where the gas−liquid mass-transfer limitation is not operative. In practice, some differences exist in the behavior of the two reactors and we attributed the differences to the liquid−solid mass-transfer coefficients that are different in the two cases. K_S in the well-mixed slurry reactor, for example, can be estimated with the correlation suggested by Sano et al.:[22]

$$\frac{Sh}{F_S} = \frac{K_S d_P}{D F_S} = 2 + 0.4 Re^{1/4} Sc^{1/3} \tag{31}$$

with

$$Re = \frac{\mathrm{Pow} d_P{}^4 \rho^3}{\mu^3}; \quad Sc = \frac{\mu}{\rho_L D} \tag{32}$$

The values obtained by using this correlation have been imposed in the run simulation (runs A1−A5). It changes in the range of $(1.2-1.8) \times 10^{-2}$ cm/s.

Other correlations have been proposed in the literature respectively by Wakao and Funazkri[20] and by Sherwood et al.[21] for a liquid flowing across a catalytic bed as it occurs in the STLR reactor (see Figure 1).

$$Sh = \frac{K_S d_P}{D} = 2 + 1.1 (Re)^{0.6} (Sc)^{1/3}$$

relation from Wakao and Funazkri[20] (33)

$$Sh = \frac{K_S d_P}{D} = 1.17 (Re)^{0.585} \sqrt[3]{Sc}$$

relation from Sherwood et al.[21] (34)

where

$$Re = \frac{d\mathrm{p} G}{\mu} \qquad Sc = \frac{\mu}{\rho_L D}$$

Since K_S seems to have a dramatic importance for the STRL reactor, this parameter being about 1 order of magnitude less than the parameter found for the slurry reactor, we have determined this parameter from both relations found in the literature and mathematical regression on the experimental runs. The obtained values are reported in Table 5 for a useful comparison. As can be seen, the agreement between the values obtained in the different mentioned ways is satisfactory. Reaction rates, in both of the reactors used, are also limited by internal particle diffusion, as can be seen in Figure 15, where, the evolution with time of the effectiveness factors η are reported for respectively run

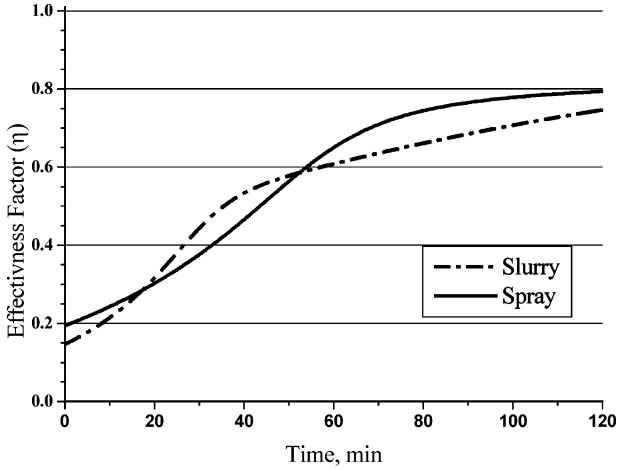

Figure 15. Catalyst effectiveness factor as a function of time for slurry and spray reactors.

A3 and run B2. A similar trend has been obtained in the two cases. As can be seen, initial values of η are very low as a consequence of both the very low isobutene diffusion coefficient in the liquid phase and the size of the catalyst particles.

In conclusion, we have demonstrated in this work that it is possible to do a gas−liquid−solid reaction in a STLR reactor, provided that the gaseous reagent has a good solubility in the liquid one and that the liquid can easily be dispersed by an efficient spray nozzle in very small droplets. Saturation of the drops is achieved, in this case, in a relatively small volume, the mass-transfer rate being very fast. Saturated liquid is then fed to the catalytic bed that could be located internally or externally with respect to the collected liquid pool. For this type of reactor the geometrical arrangement of the catalytic bed seems very important, strongly affecting the liquid−solid mass-transfer rate. The relative amount of liquid and solid filling the reactor is also very important. As many variables are involved in the optimization of this type of reactor this aspect requires to be further deepened with the help of other experimental data and more suitable fluid dynamic models.

In conclusion, the main advantage of the STLR reactors consists of the fact that these reactors can operate in the condition of intrinsic safety because no internal stirring devices are used. In fact, spray tower loop reactors have found success in gas−liquid reactions such as ethoxylation and propoxylation that present safety problems. Other important advantages are the absence of gas hold-up and the possibility of realizing a flexible modular structure in which any module has a distinct function and can easily be designed. It is possible to recognize in this structure (i) the mass-transfer zone for the liquid saturation, (ii) the liquid reservoir, (iii) the heat exchanger, and (iv) the catalyst basket.

List of Symbols

a_L = gas−liquid interfacial area (cm^2/cm^3)
a_S = liquid−solid interfacial area (cm^2/cm^3)
β_L = overall gas−liquid mass-transfer coefficient (1/s)
χ = association paramenter of the solvent, equal to 1 for unassocied solvents
C_{Bs} = concentration of monomer at the solid surface (mol/cm^3)
$C_{cat,}$ = concentration of catalyst in the bulk liquid (g/cm^3)
C_{CO_2} = carbon dioxide concentration (mol/cm^3)
$C^*_{CO_2}$ = saturation concentration of carbon dioxide (mol/cm^3)
C_{Ds} = concentration of dimer at the solid surface (mol/cm^3)
C_I = concentration of isobutene at the gas−liquid interface (mol/cm^3)
C_{Ib} = concentration of isobutene in the bulk liquid (mol/cm^3)
C_{Is} = concentration of isobutene in the bulk solid (mol/cm^3)
C_{Ms} = concentration of monomer at the solid surface (mol/cm^3)
C_{Ps} = concentration of *p*-cresol at the solid surface (mol/cm^3)
d_P = catalyst particle diameter (cm)
D = diffusion coefficient (cm^2/s)
D_{eff} = effective diffusion coefficient for isobutene (cm^2/s)
$D_{isob/p-cresol}$ = molecular diffusion coefficient of isobutene in *p*-cresol (cm^2/s)
D_{CO_2/H_2O} = molecular diffusion coefficient of carbon dioxide in water (cm^2/s)
D_{12} = molecular diffusion coefficient of 1 in 2 (cm^2/s)
D_{32} = Sauter mean drop diameter (μm)
ϵ_p = tortuosity factor
Φ = Thiele modulus
F_S = shape factor of the particles
G = superficial mass velocity ((cm^2 s)/g)
$\overline{\gamma_I}$ = activity coefficient of isobutene in the reaction mixture
$\overline{\gamma_I^{inf}}$ = activity coefficient of isobutene, at infinite dilution, in the reaction mixture
K_{e1} = equilibrium constant for reaction P + I > M
K_{e2} = equilibrium constant for reaction M + I > BHT
k_i = kinetic constant for ith reaction (cm^4/(s mol))
K_L = liquid mass transport coefficient (cm/s)
K_S = solid mass transport coefficient (cm/s)
μ = viscosity (g/(cm s))
M_2 = molecular weight of the solvent (g/mol)
η = catalyst effectiveness factor
n_i = moles of ith component
Pow = energy supplied to the slurry, by stirring, per unit mass (cm^2/s^2)
r_i = rate of ith reaction (mol/(s cm^3))
Re = Reynolds number
ρ_L = liquid density (g/cm^3)
R_P = particle radius (cm)
Sc = Schmidt number
Sh = Sherwood number
S_{spec} = Catalyst specific surface area (cm^2/g)
t = time (s)
T = temperature (K)
V_B = molar volume of the diffusing solute (cm^3/mol)
V_L = liquid-phase volume (cm^3)
x_i = molar fraction of ith component

Literature Cited

(1) Brogren, C.; Karlssonn, H. T. Modeling the Absorption of SO_2 in a Spray Scrubber Using the Penetration Theory. *Chem. Eng. Sci.* **1997**, *52* (18), 3085−3099.

(2) Pigford, R. L.; Pyle, C. Performance Characteristic of Spray-Type Absorption Equipment. *J. Ind. Eng. Chem.* **1951**, *43*, 1649−1662.

(3) Metha, K. C.; Sharma, M. M. Mass Transfer in Spray Columns. *Br. Chem. Eng.* **1970**, *15*, 1440−1558.

(4) Pinilla, E. A.; Diaz, J. M.; Coca, J. Mass Transfer and Axial Dispersion in a Spray Tower for Gas−Liquid Contacting. *Can. J. Chem. Eng.* **1984**, *62*, 617−22.

(5) Sirignano, W. A. *Fluid Dynamics and Transport of Droplets and Sprays*; Cambridge University Press: Cambridge, U.K., 1999.

(6) Dimiccoli, A.; Di Serio, M.; Santacesaria, E. Mass Transfer and Kinetic in Spray-Tower-Loop Absorber and Reactors. *Ind. Eng. Chem. Res.* **2000**, *39*, 4082−4093.

(7) Yeh, N. K.; Rochelle, G. T. Liquid-Phase Mass Transfer in Spray Contactors. *AICHE J.* **2003**, *49*, 2363−2373.

(8) Dimiccoli A.; Di Serio M.; Santacesaria E. Key Factors in Ethoxylation and Propoxylation Technology *Proceedings of the 5th World Surfactants Congress*, Florence, Italy, May 29−June 2, 2000; pp 114−125.

(9) Santacesaria, E.; Di Serio, M.; Iengo, P. Mass Transfer and Kinetics in Ethoxylation Spray Reactors. *Chem. Eng. Sci.* **1999**, *54*, 1499−1504.

(10) Santacesaria E.; Di Serio M.; Iengo, P. *Reaction Kinetics and the Development of Catalytic Processes*; Froment, Waugh, Eds.; Studies in Surface Science and Catalysis 122; Elsevier: Amsterdam, 1999; pp 267−274.

(11) Santacesaria, E.; Di Serio, M.; Lisi, L.; Gelosa, D. Kinetics of Nonylphenol Polyethoxylation Catalyzed by Potassium Hydroxide. *Ind. Eng. Chem. Res*. **1990**, *29*, 719−725.

(12) Santacesaria, E.; Silvani, R.; Wilkinson, P.; Carrà, S. Alkylation of *p*-Cresol with Isobutene Catalyzed by Cation-Exchange Resins: A Kinetic Study. *Ind. Eng. Chem. Res.* **1988**, *27*, 541−548.

(13) Yadav G. D.; Thorat, T. S. Kinetics of Alkylation of *p*-Cresol with Isobutylene Catalyzed by Sulfated Zirconia. *Ind. Eng. Chem. Res.* **1996**, *35*, 721−731.

(14) Lide, D. R.; Frederikse, H. P. R. *CRC Handbook of Chemistry and Phisic*, 74th ed.; CRC Press: Boca Raton, FL, 1993.

(15) Stephen, H.; Stephen, T. *Solubilities of Inorganic and Organic Compounds*; Pergamon Press: Oxford, U.K., 1963; Vol. 1, Part 1.

(16) Perry, R. H.; Green, W. *Perry's Chemical Engineers' Handbook*, 7th ed.; McGraw-Hill: New York, 1997; Vol. 2, p 330.

(17) Wilke, C. R.; Chang, P. *AIChE J.* **1955**, *1*, 264.

(18) Buzzi-Ferraris G. Metodo Automatico per Trovare l'Ottimo di una Funzione. *Ing. Chim. Ital*. **1968**, *4*, 171−187.

(19) Satterfield, C. N.; Sherwood, T. K. *The Role of Diffusion in Catalysis*; Addison-Wesley: Reading, MA, 1963.

(20) Wakao, N.; Funazkri, T. Effect of Fluid Dispersion Coefficients on Particle to Fluid Mass Transfer Coefficients in Packed Beds. Correlation of Sherwood Numbers. *Chem. Eng. Sci.* **1978**, *33* (10), 1375−1384.

(21) Sherwood, T. K.; Pigford, R. L.; Wilke, C. R. *Mass Tranfer*; McGraw-Hill: New York, 1975; p 242.

(22) Sano, Y.; Yamaguchi, N.; Adechi, T. Mass Transfer Coefficients for Suspended Particles in Agitated Vessel and Bubble Columns. *J. Chem. Eng. Jpn.* **1974**, *7* (4), 255−261.

Received for review February 22, 2005
Revised manuscript received June 29, 2005
Accepted July 12, 2005

IE050221J